

The AVO modelling volume

Brian H. Russell, Laurence R. Lines, Keith W. Hirsche¹, and Janusz Peron¹

ABSTRACT

An AVO modelling scheme is proposed in which we create a 3D volume of modelled CDP gathers by varying two physical parameters, one in the in-line direction, and one in the cross-line direction. This 3D volume is then processed using conventional AVO analysis techniques, and the results are interpreted using time or structure slices. Two illustrative examples are presented, one involving P-wave velocity change versus S-wave velocity change, and the other involving P-wave velocity change versus thickness change. Future research applications will involve the use of this method to map pressure versus saturation changes for the use of AVO methods to determine time-lapse changes in a heavy oil reservoir.

INTRODUCTION

AVO analysis generally involves the computation of several independent attributes from prestack seismic data, such as near and far stack, intercept and gradient, on μ -rho and λ -rho. However, due to the non-uniqueness of seismic data, there are a large number of possible geological models that can be postulated that will all fit the results of such an analysis. For this reason, it is important to perform modelling to try and better understand the information contained in observed seismic data. This is traditionally done by creating a model from the observed well logs, perturbing a single parameter, and observing the results. In this paper, we propose a straightforward method for creating multiple AVO models, which we will call the AVO modelling volume. The 3D AVO modelling volume is created by choosing two physical parameters of interest, and allowing each to change in a systematic fashion, one in the in-line direction of a 3D volume, and the other in the cross-line direction. This creates a cube of multi-offset AVO models, each with a different combination of physical parameters. This cube can then be processed in a traditional fashion to compute two attributes, say intercept and gradient, and the results can then be displayed in data slice format, where the in-line direction can be related to changes in the first parameter, and the cross-line direction can be related to changes in the second parameter. This paper will look at several data examples of this method, and will propose future applications in which this method will be used.

CREATING THE AVO MODELLING VOLUME

Our first decision when creating an AVO modelling volume is to decide which two parameters to change. They could consist of two elastic parameters, chosen from P-wave velocity, S-wave velocity, Poisson's ratio, and density, or two parameters that affect these elastic values, such as porosity, saturation, permeability, temperature or pressure. Obviously the latter choices require analytical expressions that tie changes in these parameters to changes in the underlying elastic constants used in the

¹ Hampson-Russell Software Services Ltd., Calgary, Alberta, Canada.

modelling of the AVO changes. For example, the Biot-Gassmann equations could be used to model porosity versus saturation changes, whereas a measured table of values of elastic parameter changes versus pressure change could be used to model reservoir conditions. Other parameters that are of interest, since they affect the seismic response, are layer thickness, seismic bandwidth, and phase rotation. Finally, you may want to consider the effects of different modelling algorithms, such as primaries-only modelling versus the effect of adding converted waves. In this latter case, it is useful to create two separate modelling cubes, and look at the differences between the two.

A FIRST EXAMPLE: P-WAVE VELOCITY VERSUS S-WAVE VELOCITY

As a first example of the AVO modelling volume, we will perturb the three layer log suite shown in figure 1. This log consists of a first and third layer of equal elastic parameters ($\rho = 2.11 \text{ g/cc}$, $V_P = 2250 \text{ m/s}$, $V_S = 1125 \text{ m/s}$, $\sigma=1/3$) and a second layer which will be allowed to change.

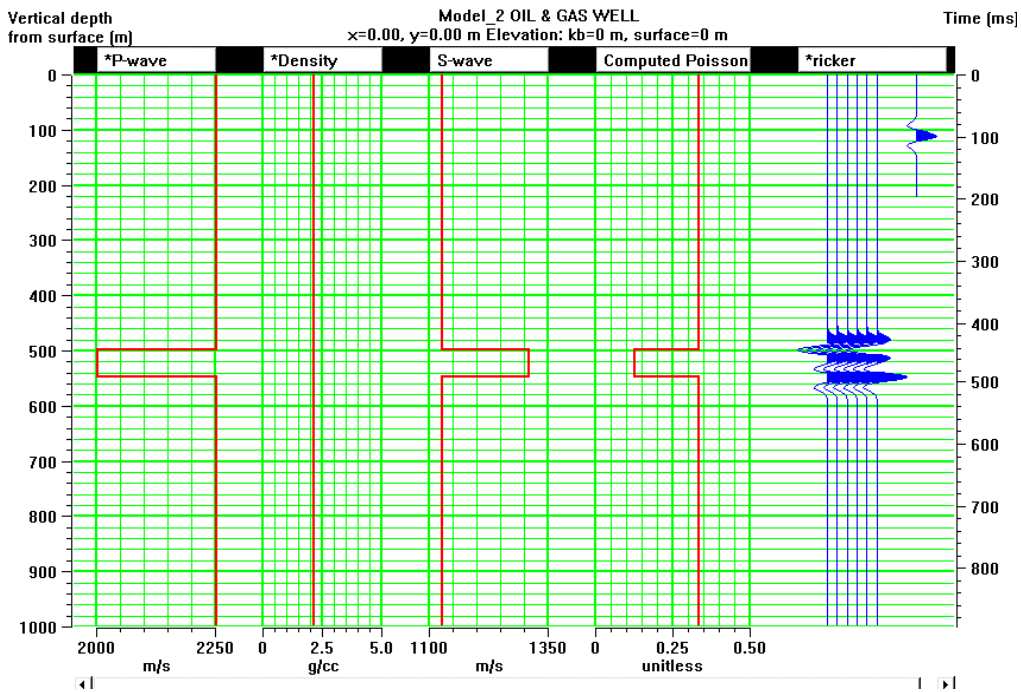


Figure 1. Logs used in the AVO modelling volume computations, where the zero-offset synthetic is shown on the right.

The two parameters to be changed will be P-wave velocity and S-wave velocity, and the density will be held constant in all layers to minimize its effect. The layer thickness was chosen to be large (50 meters) to minimize the effect of thin bed tuning, and a 25 Hertz Ricker wavelet was used in the modelling process. Also, the far offset used was 500m, which is equal to the depth to the top layer. A 6x6 cube of modeled gathers was then created by allowing P-wave velocity to vary from 2000m/s to 2500m/s in increments of 100m/s, and S-wave velocity to vary from 1000m/s to 1250m/s in increments of 50m/s. Note that this will create 36 gathers with V_P/V_S ratios varying from 2/5 to 5/8, or Poisson's ratios, σ , varying from 0.18 to 0.40. As a

reminder, recall that Poisson's ratio is a function of the Vp/Vs ratio and is specifically defined as:

$$\sigma = \frac{\left(\frac{V_P}{V_S}\right)^2 - 2}{2\left(\frac{V_P}{V_S}\right)^2 - 2} \quad (1)$$

Table 1 shows the Poisson's ratio value for various pairs of Vp and Vs values, where we have used a 50 m/s increment for Vp and a 25 m/s increment for Vs. Notice that this gives an 11x11 grid, whereas our first model uses only every second one of these values.

Table 1. The computed Poisson's ratio for various combinations of P-wave and S-wave velocity, where P-wave velocity is annotated vertically on the left side of the table and S-wave velocity is annotated on the top vertical line. Both velocities are in m/sec.

	1000	1025	1050	1075	1100	1125	1150	1175	1200	1225	1250
2000	0.33	0.32	0.31	0.30	0.28	0.27	0.25	0.24	0.22	0.20	0.18
2050	0.34	0.33	0.32	0.31	0.30	0.28	0.27	0.26	0.24	0.22	0.20
2100	0.35	0.34	0.33	0.32	0.31	0.30	0.29	0.27	0.26	0.24	0.23
2150	0.36	0.35	0.34	0.33	0.32	0.31	0.30	0.29	0.27	0.26	0.24
2200	0.37	0.36	0.35	0.34	0.33	0.32	0.31	0.30	0.29	0.28	0.26
2250	0.38	0.37	0.36	0.35	0.34	0.33	0.32	0.31	0.30	0.29	0.28
2300	0.38	0.38	0.37	0.36	0.35	0.34	0.33	0.32	0.31	0.30	0.29
2350	0.39	0.38	0.38	0.37	0.36	0.35	0.34	0.33	0.32	0.31	0.30
2400	0.39	0.39	0.38	0.37	0.37	0.36	0.35	0.34	0.33	0.32	0.31
2450	0.40	0.39	0.39	0.38	0.37	0.37	0.36	0.35	0.34	0.33	0.32
2500	0.40	0.40	0.39	0.39	0.38	0.37	0.37	0.36	0.35	0.34	0.33

The modelling algorithm used was a primaries-only scheme in which the amplitudes were computed using the Zoeppritz equations, ray-tracing was used to compute the event traveltimes, and the final model was created by applying an NMO correction. The advantage of this modelling scheme is that it is fast and efficient, but the disadvantages are that we are ignoring the effects of converted waves, anelasticity, and anisotropy. As was mentioned earlier, these are all options that can be used in further modelling examples.

Figure 2 shows the results of the modelling for all 36 models, with Vp changing in the vertical direction, and Vs changing in the horizontal direction. Although the expected trends are present in Figure 2, with Vp controlling the zero-offset reflection coefficient, and Vp/Vs controlling the change in amplitude as a function of offset, there is a lot of information to assimilate in this figure.

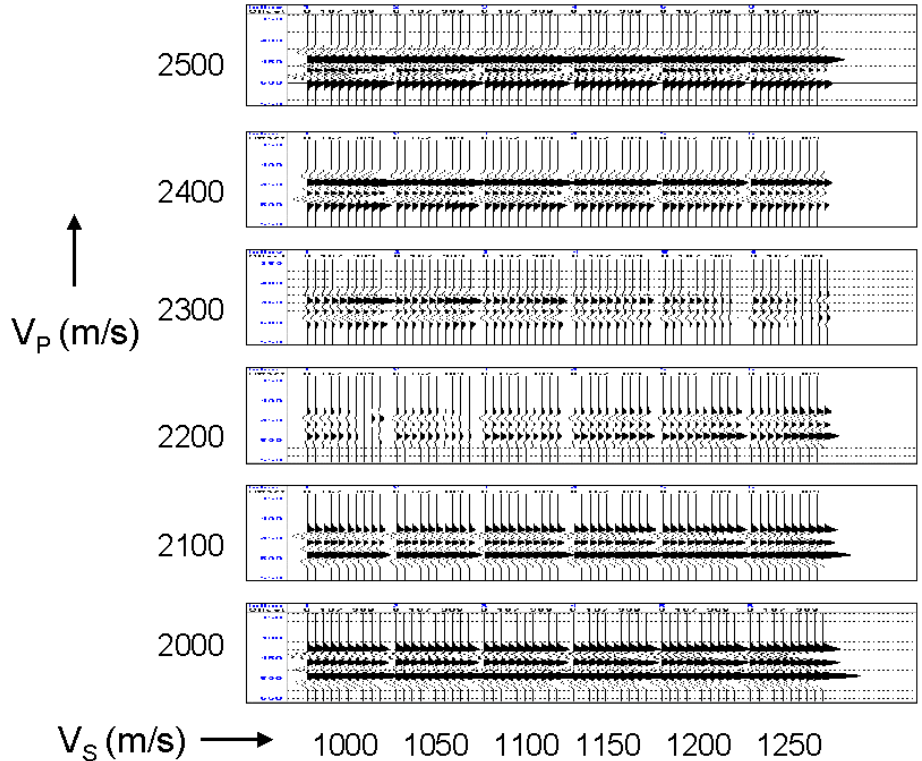


Figure 2. The results of the first AVO modelling volume, where the in-line (horizontal) direction represents change in S-wave velocity and the cross-line direction (vertical) represents changes in P-wave velocity.

The next step is therefore to process the modelling cube for two separate attributes and analyze these results. Although, as was mentioned earlier, there are many possible pairs of attributes that could be chosen, we decided to use the intercept and gradient attributes, as they are the most common attributes used in current practice. The processed volumes were then sliced at a time of 444 msec, which corresponds to the maximum on the first event (trough or peak). The slices through the intercept and gradient volumes are shown in Figures 3(a) and 3(b), respectively. Notice that the intercept slice shows a horizontal striping, and the gradient slice shows roughly diagonal striping. Let us analyze the reasons for this, by reviewing the basic mathematics behind the AVO attribute process.

The intercept and gradient can be written in linearized form as (Aki and Richards, 1980, Wiggins et al, 1983):

$$R(\theta) = A + B \sin^2 \theta + C \sin^2 \theta \tan^2 \theta \tag{2}$$

The third term, C, is small for angles less than 30 degrees, and is usually dropped, although this is not a good idea for long offset data. It can be written:

$$C = \frac{1}{2} \frac{\Delta V_P}{V_P} \quad (3)$$

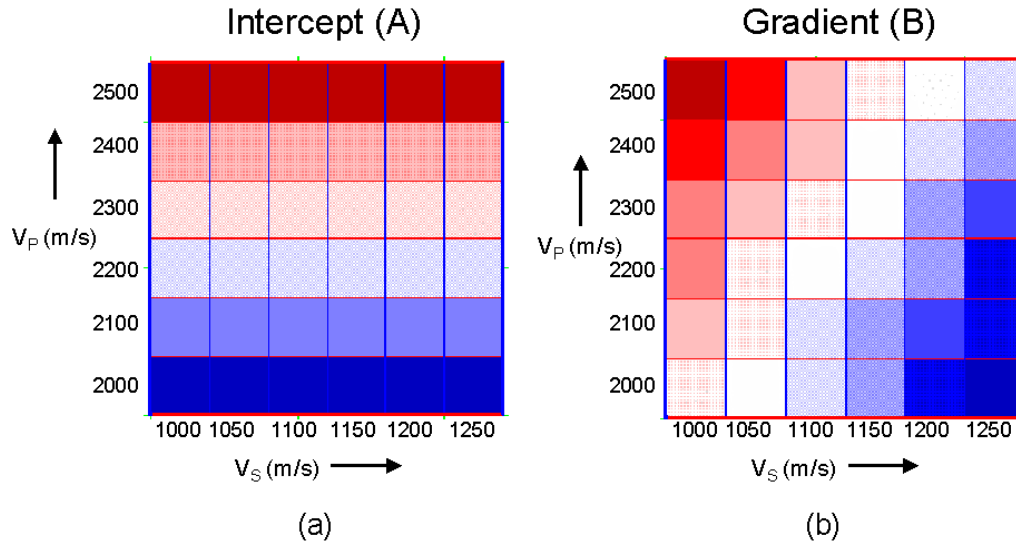


Figure 3. Time slices from the (a) intercept and (b) gradient volumes computed from the gathers shown in Figure 2. Red represents positive values and blue represents negative values.

In our case, we are more interested in the A term, which is called the intercept, and the B term, which is called the gradient. The intercept A represents the zero-offset P-wave reflectivity, which can be written

$$A = R_{P0} = \frac{1}{2} \left[\frac{\Delta V_P}{V_P} + \frac{\Delta \rho}{\rho} \right] \quad (4)$$

where ΔV_P and $\Delta \rho$ are the changes in P-wave velocity and density across the layer boundaries, and V_P and ρ are the average P-wave velocity and density across the layer boundaries. Since there is no change in density in our model, the reflection coefficient can be written solely as the change in P-wave velocity, or:

$$A = R_{P0} = \frac{1}{2} \left[\frac{\Delta V_P}{V_P} \right] \quad (5)$$

We can therefore see the horizontal stripes in Figure 3(a) reflect this vertical change in P-wave velocity seen in the modelling cube.

Let us now look at the results of the gradient analysis. The gradient term in the Aki-Richards linearized equation can be written as:

$$B = \frac{1}{2} \frac{\Delta V_P}{V_P} - 4 \left(\frac{V_S}{V_P} \right)^2 \frac{\Delta V_S}{V_S} - 2 \left(\frac{V_S}{V_P} \right)^2 \frac{\Delta \rho}{\rho} \quad (6)$$

If we assume that the V_P/V_S ratio is equal to 2, the gradient simplifies to:

$$B = R_{P0} - 2R_{S0} \quad (7)$$

where $R_{S0} = \frac{1}{2} \left[\frac{\Delta V_S}{V_S} + \frac{\Delta \rho}{\rho} \right]$

Again, noting that $\Delta \rho / \rho = 0$ in our example, the shear wave reflectivity simplifies to:

$$R_{S0} = \frac{1}{2} \left[\frac{\Delta V_S}{V_S} \right] \quad (8)$$

Therefore, the gradient is responding to the difference between changes in P-wave velocity and twice the changes in S-wave velocity (only approximately, since the V_P/V_S ratio is not constant).

A common method of AVO analysis is to produce weighted sums or differences of the intercept and gradient. Physically, if we use the above simplification of the gradient, we see that:

$$\frac{A+B}{2} = R_{P0} - R_{S0} \quad (9)$$

and:

$$\frac{A-B}{2} = R_{S0} \quad (10)$$

The sum $A+B$ can also be thought of as the scaled change in Poisson's ratio, if we start with Shuey's linearized approximation, involving V_P , ρ and Poisson's ratio σ . This will be discussed later.

We thus created the sum and difference of the intercept and gradient slices shown in Figure 3. (Note that this could be done either using the slices themselves, or by combining the volumes and re-slicing. In this case, both methods produce the same result, but in general it is advisable to combine the volumes and re-slice). The sum and difference plots are shown in Figures 4(a) and 4(b) respectively. Notice that the summed slice shows perfect diagonals since it now represents the difference between changes in P-wave velocity and S-wave velocity. The difference slice shows vertical striping rather than horizontal striping, since it is responding to changes in the S-wave velocity. The vertical striping is not perfect since the V_P/V_S ratio is not constant and

equation (10) is only strictly valid when $V_p/V_s = 2$ and the third term in equation (2) is negligible. We do not fully understand why the diagonal striping of the summed attributes was so perfect, since equation (9) is also an approximation.

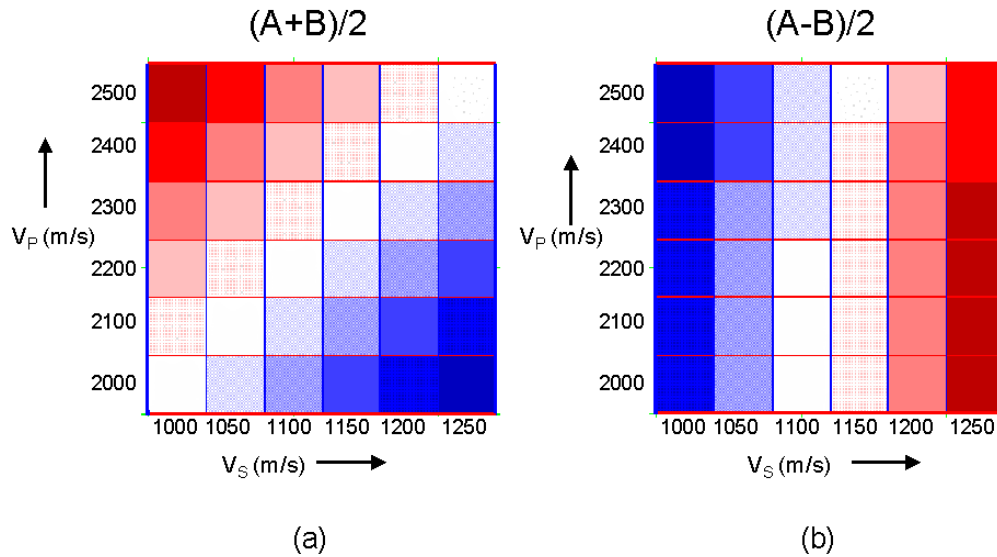


Figure 4. Time slices of the (a) sum and (b) difference of the intercept and gradient slices shown in Figure 3. Red represents positive values and blue represents negative values.

A TUNING THICKNESS EXAMPLE

In our second example, we will use changes in P-wave velocity versus bed thickness change. To create the V_p versus thickness change volume, the P-wave velocity was varied from 2000m/s to 2500m/s, but this time in increments of 50m/s, creating 11 separate in-lines. Since the P-wave velocity in the first and third layers was equal to 2250m/s, this meant that the sixth line would have zero reflection coefficients. Also, since only the P-wave velocity was changing, the question arose as to what to do with the S-wave velocity (and hence the associated Poisson's ratio.) It was decided to keep the S-wave velocity constant, and equal to the velocity of the first and third layers, or 1125m/s. This meant that the Poisson's ratio was effectively changed from a value of 0.27 (at $V_p=2000\text{m/s}$) to a value of 0.37 (at $V_p=2500\text{m/s}$). This is shown for each value in Table 1. Also note from Table 1 that the value of Poisson's ratio at $V_p=2250\text{m/s}$ is equal to $1/3$, which is the same value as the surrounding layers. This is an important thing to remember when looking at the upcoming figures, since it makes the change in Poisson's ratio, $\Delta\sigma$, equal to zero in the central column of the cube.

For the thickness change, it was decided to start with a layer thickness of 5m, well below tuning, and end at a thickness of 55m, well above tuning. The thickness increment was 5m, which created 11 cross-lines. (Again, we have created a perfect square of bins. There is no reason to do this, since we could just as easily have a rectangular volume, but it creates a nice display!)

The 11x11 volume of gathers was then created, again using a primaries only Zoeppritz modelling scheme, with a 25 Hz Ricker wavelet. The results were then processed through to intercept and gradient. Figure 5 shows a portion of the intercept volume, displayed in wiggle-trace format, for every second in-line. Recall that each in-line has a constant P-wave velocity and that the changes, from left to right, show bed thickening. The effect of this bed thickening is to produce different tuned seismic responses and to introduce apparent structure. We therefore picked the volume, starting with a trough on in-line 1 (when we have a drop in P-wave velocity) and changing to a peak on in-line 7 (when the P-wave velocity changes to an increase across the boundary). In-line 6, which is not shown, shows zero amplitude, and the picked structure was “phantomed” by interpolating the times between in-lines 5 and 7. Also in Figure 5, notice that the P-wave velocity from the well logs has been superimposed on Figure 5(a), or in-line 1. The thin 5m sand is obviously below tuning and the seismic trough and peak do not correspond to the actual bed boundaries.

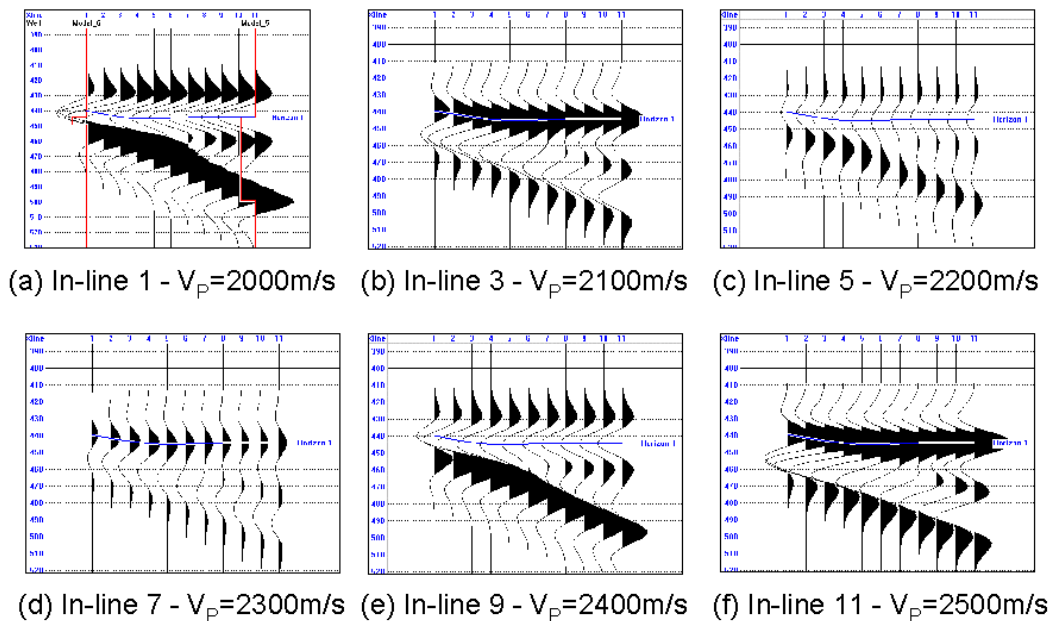


Figure 5. Every second in-line from the intercept volume created by varying P-wave velocity in the in-line direction and bed thickness in the cross-line direction. In all of the above plots, thickness increases from 5 m to 55 m as you move from left to right on the seismic displays.

Now let us look at the slices. This time the amplitudes were found at the picked time locations from Horizon 1, shown in Figure 5. Figure 6 shows the slices from the intercept and gradient stacks. Notice the vertical striping in both volumes, controlled by the changing P-wave velocity and Poisson’s ratio. At in-line 6, both are zero. This is clear for the intercept, which is being totally controlled by the P-wave velocity. But why is it equal to zero for the gradient?

To understand this, let us write down Shuey's formula for gradient (Shuey, 1985):

$$B = R_{P0}A_0 + \frac{\Delta\sigma}{(1-\sigma)^2} \quad (11)$$

where $\Delta\sigma$ is the change in Poisson's ratio across the layer boundaries, σ is the average Poisson's ratio across the layer boundaries, and:

$$A_0 = C - 2(1+C)\frac{1-2\sigma}{(1-\sigma)},$$

where

$$C = \frac{\Delta V_p / V_p}{\Delta V_p / V_p + \Delta \rho / \rho}.$$

A common simplification of equation (11), which was referred to earlier, is to set the average value σ to 1/3, which is equivalent to a Vp/Vs ratio of 2. Note that this leads to a much simpler equation:

$$B = -R_{P0} + \frac{4}{9}\Delta\sigma \quad (12)$$

From equation (12), you can indeed verify the alternate interpretation of A+B, as:

$$\Delta\sigma = \frac{A+B}{2.25} \quad (13)$$

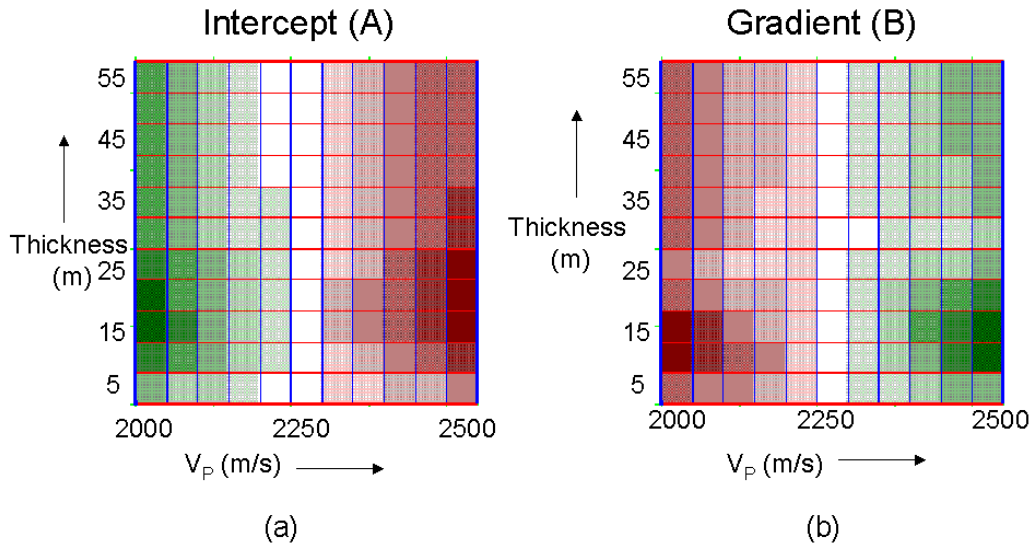


Figure 6. The structure slices at Horizon 1 (from Figure 5) from the (a) intercept and (b) gradient volumes produced from the AVO modelling volume of P-wave velocity change versus bed thickness change. Brown represents positive values and green represents negative values.

Now we are in a position to answer the earlier question. Since, as mentioned earlier, the Poisson's ratio at in-line 6 is equal to the Poisson's ratio of the overlying and underlying layers, and thus $\Delta\sigma = 0$, we can see that B must also be equal to zero for all cross-lines above in-line 6. But what is more interesting in Figure 6 is the change in the gradient and intercept as we move up the cross-line, or vertical, axis. As you can see, there are pronounced tuning effects at thicknesses between about 10m and 35m on the intercept slice, and between about 10 and 20m on the gradient slice. These models show increased amplitudes as expected. But there are several surprises. First of all, the tuning effects are different between intercept and gradient, and are different from the left to the right of the plot. Second, the tuning effects for the negative gradient seem to decrease suddenly at a thickness of 30m, and then increase again at 35m. This is an unexplained effect. However, we do not want to draw too many conclusions from this plot, since there are many complicating factors, such as the sample rate, the algorithm used to extract A and B, the fact that the third term in the linearized Aki-Richards equation was not used, and so on.

Next, let us look at Figure 7, which shows the $(A+B)/2$ result in Figure 7(a) and the $(A-B)/2$ result in Figure 7(b). Again, we must not try to read too much into these plots. But several factors are apparent. If we were to use $(A+B)/2$ as an estimate of $\Delta\sigma$, we would underestimate the change in Poisson's ratio at thicknesses below tuning (5-10m) and overestimate this value at tuning (15-30m). And, if we were to use $(A-B)/2$ as an estimate of R_{S0} , we would be wrong almost everywhere, since $R_{S0}=0$ in all cells!

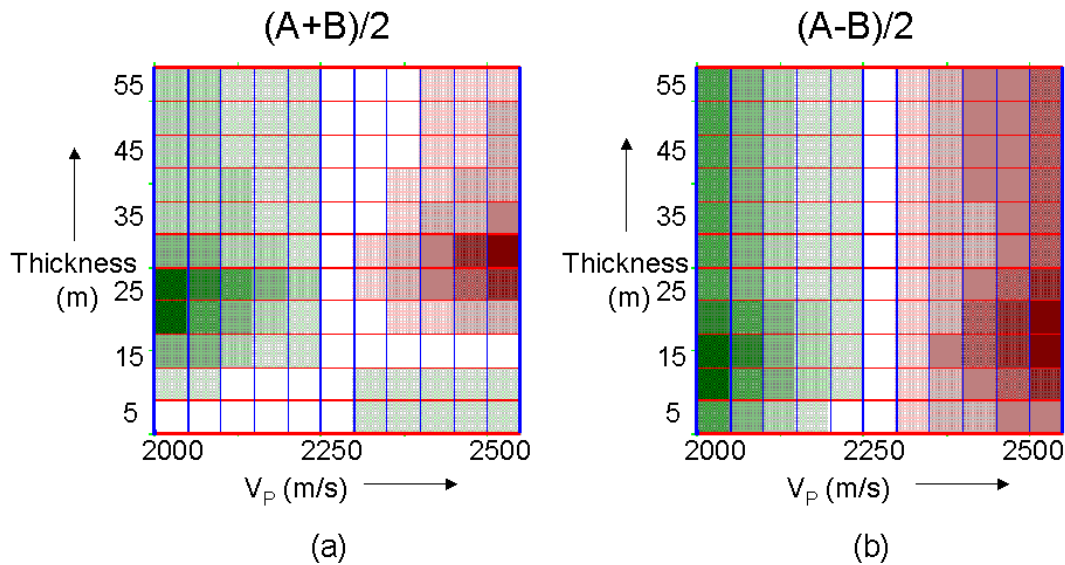


Figure 7. The structure slices from the (a) sum and (b) difference of the intercept and gradient slices shown in figure 6. Brown represents positive values and green represents negative values.

CONCLUSIONS

In this paper we have discussed a new method for two parameter AVO modelling. This method involves creating a pseudo-3D volume of modeled gathers in which variations in one parameter are changed along the in-line direction, and variations of the other parameter are changed along the cross-line direction. By treating the resulting volume as a 3D section, and processing it with standard AVO analysis techniques, subtle effects due to the different parameters are revealed that would otherwise have been difficult to visualize. Our first model, which changed P-wave velocity versus S-wave velocity, gave us a better understanding of the various intercept/gradient method. Our second example, which changed P-wave velocity against bed thickness, gave us a better understanding of tuning effects.

FUTURE WORK

Future work will involve changing pairs of reservoir parameters, such as pressure and fluid saturation, and comparing the results to the AVO analysis of gathers from a time lapse study in a heavy oil reservoir.

ACKNOWLEDGEMENTS

We wish to thank our colleagues at the CREWES Project and at Hampson-Russell Software for their support and ideas, as well as the sponsors of the CREWES Project.

REFERENCES

- Aki, K., and Richards, P.G., 1980, Quantitative seismology: Theory and methods: W.H. Freeman and Company.
- Shuey, R.T., 1985, A simplification of the Zoeppritz equations: *Geophysics*, 50, 609-614.
- Wiggins, R., Kenny, G.S., and McClure, C.D., 1983, A method for determining and displaying the shear-velocity reflectivities of a geologic formation: European Patent Application 0113944.